16th World Congress in Computational Mechanics (WCCM)
21-26 July 2024, Vancouver, Canada
A. Korobenko, M. Laforest, S. Prudhomme, R. Vaziri (Eds)

PREDICTOR-CORRECTOR SECOND-ORDER TIME-STEPPING SCHEMES FOR SOLVING WATER FLOW AND SOLUTE TRANSPORT IN UNSATURATED POROUS MEDIA

NOUR-EDDINE TOUTLINI[1,2], HAMZA KAMIL[1,2], AZZEDDINE SOULAÏMANI[1], AND ABDELAZIZ BELJADID[2,3]

[1] École de technologie supérieure
1100 Notre-Dame Ouest, Montréal, QC H3C 1K3, Canada
azzeddine.soulaimani.1@ens.etsmtl.ca

[2] Mohammed VI Polytechnic University
Lot 660, Hay Moulay Rachid Ben Guerir, 43150, Morocco
nour-eddine.toutlini.1@ens.etsmtl.ca;
hamza.kamil.1@ens.etsmtl.ca

[3] University of Ottawa
150 Louis-Pasteur Pvt, Ottawa, K1N 6N5, Ontario, Canada
beljadi@uottawa.ca

Key words: Solute transport; water flow; porous media; Richards equations; predictor-corrector scheme; finite element method

Abstract. The objective of this study is to numerically solve the coupled system of water flow and solute transport in unsaturated porous media using a noniterative predictor-corrector temporal scheme for the Richards equation and a semi-implicit temporal scheme for the advection-dispersion equation (ADE). The standard and non-standard Galerkin finite element methods are used for spatial discretization. Three different techniques are proposed to calculate the pressure head in the Levrett equation. These techniques are different in terms of the chosen shape functions in the finite element space. The proposed schemes offer distinct advantages due to the linear nature of the resulting system, facilitating easy implementation and avoiding the issues associated with the divergence of iterative schemes. We evaluated the robustness and efficacy of the suggested methods using a computational experiment to simulate soil salinity and water flow in loamy soil. We compared it with data found in the literature. The results provide compelling evidence confirming the proposed methods' effectiveness and stability.

1 INTRODUCTION

Modeling water flow and solute transport through porous media is crucial for various applications, such as soil physics, hydrogeology, and agriculture. The Richards equation [1] is used for modeling water flow and is combined with the equilibrium advection-dispersion equation

for solute transport [13, 11] in unsaturated porous media. However, solving these equations exactly presents a considerable challenge due to the highly nonlinear relationships among the governing variables. Therefore, the use of numerical models becomes a versatile tool to solve this coupled system. Over time, several numerical models have been developed to address the complexities of the coupled system. In the literature, diverse approaches including the finite element, finite difference, and finite volume methods are employed [6, 4, 11]. Additionally, software programs have been developed to address the coupled system relevant to real experiments, such as (2D/3D) [10]. In this study, our focus will center on the finite element method, a widely utilized approach renowned for its capacity to effectively handle stiff problems. A standard and non-standard finite element method is used to describe the Richards equation which is based on solving the Leverett equation to find the pressure head and then using this pressure head to solve the mixed form of the Richards equation to find the saturation solution. Regarding the time discretization, The implicit Backward Euler and the second-order Backward differentiation formulation (BDF2) temporal schemes are commonly employed due to their ability to handle highly nonlinear functions and allow for reasonably sized time steps [4, 11]. However, it is important to note that this method may face convergence challenges in certain cases, particularly when applied to the Richards equation [13, 4, 11]. Semi-implicit techniques are generally much faster than fully implicit techniques. This speed difference arises because implicit methods involve iterative algorithms to solve the Richards equation, which inherently take longer to compute. Another alternate approach to iterative methods is using the predictor-corrector approach for solving the Richards equation. Most studies use this alternative technique based on utilizing a head-based for the Richards equation in the predictor phase and then using the mixed form in the corrector phase [15, 14]. In our study, a predictor-corrector mixed finite element scheme is proposed to solve the Richards equation, and a semi-implicit finite element method is used for the solute transport equation. The proposed predictor-corrector schemes differ from those found in existing literature, firstly, in the adoption of a mixed finite element formulation. This formulation incorporates both pressure head and saturation, utilizing second and third extrapolation formulas for the nonlinear Leverett J-function. Secondly, using different techniques to calculate the pressure head variable in the Leverett equation. Our goal in this paper is to evaluate the performance and robustness of the proposed schemes in solving the coupled system of water flow and solute transport. The remainder of the paper is structured as follows. Section 2 provides the governing equations of the coupled system. Section 3 presents the temporal schemes and the related weak formulations. Numerical results are then presented in Section 4. Section 5 provides a summary of the final remarks.

2 WATER FLOW AND SOLUTE TRANSPORT

The coupled water flow and solute transport system in unsaturated porous media is usually described using the Richards and the advection dispersion equations:

$$\begin{cases} \phi \dfrac{\partial S}{\partial t} - \nabla \cdot \left(K_s k_r \nabla \Psi + \dfrac{\partial K}{\partial z} \right) = 0, \\ \dfrac{\partial R\theta c}{\partial t} - \nabla \cdot (\theta \mathbf{D} \nabla c - c\mathbf{q}) = 0. \end{cases} \tag{1}$$

In these equations, S (-) represents the saturation of the medium, c [ML^{-3}] represents the solute concentration, θ ($\mathrm{L}^3\mathrm{L}^{-3}$) is the water content, Ψ (L) denotes the pressure head, k_r (-) is the relative hydraulic conductivity, K_s (LT^{-1}) stands for the saturated hydraulic conductivity, $K = K_s k_r$ (LT^{-1}) is the unsaturated hydraulic conductivity, $\mathbf{D}$ ($\mathrm{L}^2\mathrm{T}^{-1}$) is the dispersion tensor, $\mathbf{q}$ is the volumetric flux density (LT^{-1}). (x, z) are the Cartesian coordinates of the domain, with z (L) being positive upward and t (T) is the time. The water flux $\mathbf{q}$ in the soil is expressed using the Darcy law [7] as follows:

$$\mathbf{q} = -K \nabla (\Psi + z).$$

The system of equations (1) should be supplemented by the following initial conditions:

$$S(x, z, 0) = S_0(x, z) \text{ and } c(x, z, 0) = c_0(x, z) \text{ in } \Omega, \tag{2}$$

and the following boundary conditions:

$$\begin{cases} (S, c) & = (S_D, c_D) & \text{(Dirichlet boundary condition)}, \\ \mathbf{q} \cdot \mathbf{n} & = q_w & \text{(water flux boundary condition)}, \\ -(\theta \mathbf{D} \nabla c - \mathbf{q}c) \cdot \mathbf{n} & = q_s & \text{(solute flux boundary condition)}, \end{cases} \tag{3}$$

where $\mathbf{n}$ is the exterior unit normal vector to $\Gamma =: \partial\Omega$. The components of the dispersion tensor, $\mathbf{D}$, are expressed by the standard equations [12]:

$$\begin{aligned} D_{xx} &= D_T |\mathbf{v}| + (D_L - D_T) \frac{v_x^2}{|\mathbf{v}|} + \tau^* D_o, \\ D_{xz} &= (D_L - D_T) \frac{v_x v_z}{|\mathbf{v}|}, \\ D_{zz} &= D_T |\mathbf{v}| + (D_L - D_T) \frac{v_z^2}{|\mathbf{v}|} + \tau^* D_o, \end{aligned} \tag{4}$$

where D_L (L) is the longitudinal dispersivity and D_T (L) is the transverse one, D_o ($\mathrm{L}^2 T^{-1}$) is the molecular diffusion coefficient of the solute in free water, τ^* is the tortuosity factor and $|\mathbf{v}|$ is the absolute value of velocity vector.

The soil water retention and hydraulic conductivity are calculated using the van Genuchten model (VG) [3]:

$$S = \frac{1}{(1+\alpha_v|\Psi|_v^n)^{m_v}}$$
$$k_r = S^{\frac{1}{2}}\left[1-\left(1-S^{\frac{1}{m_v}}\right)^{m_v}\right]^2,$$

where α_v (L^{-1}) is the parameter related to the average pore size, n_v (-) is a parameter related to pore size distribution, and $m_v = 1 - \frac{1}{n_v}$ ($n_v > 1$). The pressure head is described using the Leverett J-function as follows [8, 11]:

$$\Psi = \psi_c J(S), \tag{5}$$

where J and ψ_c represent the Leverett J-function and the capillary rise function, respectively, which are stated using the VG model as follows:

$$\psi_c = \frac{1}{\alpha_v}, \qquad J(S) = -\left(S^{-\frac{1}{m_v}}-1\right)^{\frac{1}{n_v}}. \tag{6}$$

3 METHODOLOGY

3.1 TIME DISCRETIZATION

A uniform discretization is used to decompose the time interval $[0, T]$, so that,

$$t_n = n\Delta t, \quad n = 0, 1, \ldots, N, \quad \Delta t = \frac{T}{N}, \tag{7}$$

where Δt is the utilized time step. We set $S^n \approx S(t_n)$, $\Psi^n \approx \Psi(t_n)$, $c^n \approx c(t_n)$, ... for $n = 0, 1, \ldots, N$.

For the temporal discretization of the Richards equation, we propose using explicit temporal schemes by employing a predictor-corrector approach. Regarding the solute transport equation, we propose to use a semi-implicit temporal method centered on the time level $(n + \frac{1}{2})$. All the terms in the Richards equation and ADE are approximated using a second-order or third-order time stepping method centered at time level $(n + \frac{1}{2})$. These schemes are expressed as follows:
Predictor-RE:

$$\begin{cases} \Psi^{n+\frac{1}{2}} = \psi_c\left(\frac{3}{2}J(S^n) - \frac{1}{2}J(S^{n-1})\right), \\ \phi\dfrac{S^{n+1,*}-S^n}{\Delta t} = \nabla\cdot\left(K_s k_r(\Psi^{n+\frac{1}{2}})\nabla\Psi^{n+\frac{1}{2}} + \dfrac{\partial K^{n+\frac{1}{2}}}{\partial z}\right). \end{cases} \tag{8}$$

Corrector-RE:

$$\begin{cases} \Psi^{n+\frac{1}{2}} = \psi_c\left(\frac{3}{8}J(S^{n+1,*}) + \frac{6}{8}J(S^n) - \frac{1}{8}J(S^{n-1})\right), \\ \phi\dfrac{S^{n+1}-S^{n+1,*}}{\Delta t} = \nabla\cdot\left(K_s k_r(\Psi^{n+\frac{1}{2}})\nabla\Psi^{n+\frac{1}{2}} + \dfrac{\partial K^{n+\frac{1}{2}}}{\partial z}\right). \end{cases} \tag{9}$$

Semi-implicit-ADE:

$$\frac{R^{n+1}\theta^{n+1}c^{n+1} - R^n\theta^n c^n}{\Delta t} = \nabla \cdot \left[\theta^{n+1}\mathbf{D}^{n+1}\left(\frac{1}{2}\nabla c^{n+1} + \frac{1}{2}\nabla c^n\right) - \mathbf{q}^{n+1}\left(\frac{1}{2}c^{n+1} + \frac{1}{2}c^n\right)\right]. \tag{10}$$

The time discretization formulation used for the numerical treatment of the mixed form of the Richards equation in both the predictor and corrector stages is of a second-order truncation error. The order of accuracy of the extrapolation method used to approximate the Leverett J-function is $O(\Delta t^2)$ at the predictor phase (8) and $O(\Delta t^3)$ at the corrector phase (9). We highlight two primary advantages that arise from the suggested approach. Firstly, it is easy to implement. Secondly, no iterative technique is required to solve the system of equations.

3.2 SPACE DISCRETIZATION

The domain Ω is uniformly partitioned into disjoint triangles τ by $\mathcal{M}_h$, so that

$$\bar{\Omega} = \bigcup_{\tau \in \mathcal{M}_h} \tau. \tag{11}$$

The mesh size h for each element is determined as the maximum among all element sizes h_τ within the partition $\mathcal{M}_h$. The conventional finite element space, V_h, is defined by

$$V_h = \{w_h \in C^0(\Omega, \mathbb{R}) : w_h|_\tau \in P_k,\ \forall \tau \in \mathcal{M}_h\} \subset H^1(\Omega), \tag{12}$$

where P_k represents the space of polynomials on any element κ with degree less than or equal to k. The resulting semi-discrete (in space) weak formulation of the equations (8)-(10) is obtained by multiplying each equation by a test function $w_h \in V_h$ and integrating over the domain Ω and it reads as follows:

Predictor-RE: Given an initial approximation $(\Psi_h^0, S_h^0) \in V_h \times V_h$ and suitable initialization $(\Psi_h^1, S_h^1) \in V_h \times V_h$, find $(\Psi_h^{n+\frac{1}{2}}, S_h^{n+1,*}) \in V_h \times V_h$ such that:

$$\begin{cases} \displaystyle\int_\Omega \Psi_h^{n+\frac{1}{2}} w_h \, d\Omega = \int_\Omega \psi_c \left(\frac{3}{2}J(S_h^n) - \frac{1}{2}J(S_h^{n-1})\right) w_h \, d\Omega, \\ \displaystyle\int_\Omega \phi_h \left(\frac{S_h^{n+1,*} - S_h^n}{\Delta t}\right) w_h \, d\Omega + \int_\Omega \left[\left(K_s k_r(\Psi_h^{n+\frac{1}{2}})\nabla \Psi_h^{n+\frac{1}{2}} + \frac{\partial K_h^{n+\frac{1}{2}}}{\partial z}\right)\right] \cdot \nabla w_h \, d\Omega \\ \displaystyle + \int_\Gamma q_w \cdot w_h \, d\Gamma = 0 \qquad \forall w_h \in V_h. \end{cases} \tag{13}$$

Corrector-RE: Given an initial approximation $(\Psi_h^0, S_h^0) \in V_h \times V_h$ and suitable initialization $(\Psi_h^1, S_h^1) \in V_h \times V_h$, find $(\Psi_h^{n+\frac{1}{2}}, S_h^{n+1}) \in V_h \times V_h$ such that:

$$\begin{cases} \displaystyle\int_\Omega \Psi_h^{n+\frac{1}{2}} w_h \, d\Omega = \int_\Omega \psi_c \left(\frac{3}{8} J(S_h^{n+1,*}) + \frac{6}{8} J(S_h^n) - \frac{1}{8} J(S_h^{n-1}) \right) w_h \, d\Omega, \\ \displaystyle\int_\Omega \phi_h \left(\frac{S_h^{n+1} - S_h^{n+1,*}}{\Delta t} \right) w_h \, d\Omega + \int_\Omega \left[\left(K_s k_r(\Psi_h^{n+\frac{1}{2}}) \nabla \Psi_h^{n+\frac{1}{2}} + \frac{\partial K_h^{n+\frac{1}{2}}}{\partial z} \right) \right] \cdot \nabla w_h \, d\Omega \\ \displaystyle + \int_\Gamma q_w \cdot w_h \, d\Gamma = 0 \qquad \forall w_h \in V_h. \end{cases} \tag{14}$$

Semi-implicit-ADE: with a suitable approximation of the initial solution $c_h^0 \in V_h$, determine $c_h^{n+1} \in V_h$ such that:

$$\begin{cases} \displaystyle\int_\Omega \left(\frac{R_h^{n+1} \theta_h^{n+1} c_h^{n+1} - R_h^n \theta_h^n c_h^n}{\Delta t} \right) w_h \, d\Omega + \int_\Omega \left[\theta_h^{n+1} \mathbf{D}_h^{n+1} \left(\frac{1}{2} \nabla c_h^{n+1} + \frac{1}{2} \nabla c_h^n \right) \right. \\ \left. - \mathbf{q}_h^{n+1} \left(\frac{1}{2} c_h^{n+1} + \frac{1}{2} c_h^n \right) \right] \cdot \nabla w_h \, d\Omega + \displaystyle\int_\Gamma q_c \cdot w_h \, d\Gamma = 0 \qquad \forall w_h \in V_h. \end{cases} \tag{15}$$

As an initial step, we take into consideration the following initial conditions: $S_h^0 = \mathbf{\Pi}_h S_0 \in V_h$ and $c_h^0 = \mathbf{\Pi}_h c_0 \in V_h$. $\mathbf{\Pi}_h : H_0^1(\Omega) \to V_h$ represents the standard projection operator. The second step of the solution (S_h^1, c_h^1) is calculated employing the explicit temporal scheme used in [4, 13] for the Richards equation and the Backward Euler method (BDF1) for the advection-dispersion equation. In the following, we will discuss three proposed schemes to solve the Leverett equation in the predictor and corrector stages of the Richards equation. For simplicity, the discussion will be focus just on the Leverett equation in the predictor step (8) and the same analogy can be done for the corrector step. These schemes are different in terms of the chosen finite element space V_h:

1 Richards equation with continuous linear functions (RE-CP):
The first method involves selecting Ψ_h as a continuous linear function within each element Ω^e, and then the weight function w_h is also linear in each element Ω^e, i.e., the polynomial space is of order $k = 1$ (P_1). It amounts to solving the following equation:

$$\int_{\Omega^e} \Psi_h^{n+\frac{1}{2}} w_h \, d\Omega = \int_{\Omega^e} \psi_c \left[\frac{3}{2} J(S_h^n) - \frac{1}{2} J(S_h^{n-1}) \right] w_h \, d\Omega \quad \text{for all} \quad w_h \text{ linear and continuous.} \tag{16}$$

2 Richards equation with constant functions and 3 Gauss points (RE-3DP):
Here, the calculation of the variable$\Psi_h^{n+\frac{1}{2}}$ in the Richards equation of the system (8) needs

two steps: the first one is to choose the auxiliary term $\tilde{\Psi}_h^{n+\frac{1}{2}}$ as a constant in each element, i.e., the finite element space V_h is of order zero ($k = 0$). We use the Gaussian quadrature rule in 3 points to calculate the integration equation, so that:

$$\int_{\Omega^e} \tilde{\Psi}_h^{n+\frac{1}{2}} w_h \, d\Omega = \int_{\Omega^e} \psi_c \left(\frac{3}{2} J(S_h^n) - \frac{1}{2} J(S_h^{n-1}) \right) w_h \, d\Omega \qquad \text{for all} \quad w_h \text{ constant.} \tag{17}$$

Then, we use a smoothed technique to find the term $\Psi_h^{n+\frac{1}{2}}$, i.e.:

$$\int_{\Omega} \Psi_h^{n+\frac{1}{2}} w_h \, d\Omega = \int_{\Omega} \tilde{\Psi}_h^{n+\frac{1}{2}} w_h \, d\Omega \qquad \text{for all} \quad w_h \text{ linear and continuous.} \tag{18}$$

3 Richards equation with constant functions and Gauss point (RE-1DP):
This latest approach is similar to the earlier RE-3DP method. The difference lies in the computation of equation (18). Unlike the previous method which employed the Gaussian quadrature rule with 3 points, this approach uses only one Gauss point, so that:

$$\tilde{\Psi}_h^{n+\frac{1}{2}} = \frac{1}{|\Omega^e|} \left[\psi_c(x^e) \left(\frac{3}{2} J(S_h(x^e)) - \frac{1}{2} J(S_h(x^e)) \right) \right], \tag{19}$$

where x^e and $|\Omega^e|$ represent the centroid and the area of the element Ω^e, respectively. and then we use a smoothed technique to find the term $\Psi_h^{n+\delta}$, i.e.:

$$\int_{\Omega} \Psi_h^{n+\frac{1}{2}} w_h \, d\Omega = \int_{\Omega} \tilde{\Psi}_h^{n+\frac{1}{2}} w_h \, d\Omega \quad \text{for all} \quad w_h \text{ linear and continuous.} \tag{20}$$

We should note that for the solute transport equation, the finite element space $V_h$is chosen to be of order 1 (i.e. $k = 1$). To address the issue of oscillatory solutions, we utilized a mass lumping technique as done in previous studies such as in [11, 13]. In particular, we implemented the row-sum technique, which consists of summing all the terms in the mass matrix. This method was selected for its simplicity and proved to be effective in diminishing oscillations.

4 NUMERICAL RESULTS

In this section, two-dimensional numerical experiments will be conducted to evaluate the performance of the proposed schemes. The numerical test is performed using an Intel(R) Core(TM) i7-6700T, 2.80GHz, 2208 Mhz, 4 Core(s), 8 Logical Processor(s). The implementation is carried out using the finite element platform FreeFem++ [9].

4.1 2D INFILTRATION TEST

In this first test, we aim to evaluate the accuracy and efficiency of the proposed schemes by adopting analytical solution of the Richard equation. Focusing solely on the predictor phase, we apply the RE-CP, RE-3DP, and RE-1DP techniques to determine the variable $\Psi^{n+\frac{1}{2}}$ in the

Leverett equation. The test is evaluated in a square domain of length $L = 15.24\ m$. The Gardner model is used to express the Leverett J-function and the capillary rise function [2]. The soil domain is subject to the following initial and boundary conditions:

$$\begin{cases} \Psi(x, L, t) = \dfrac{1}{\alpha_v} \log\left[\xi + (1-\xi)\sin\left(\dfrac{\pi x}{L}\right)\right], \\ \Psi(0, z, t) = \Psi(L, z, t) = \Psi(x, 0, t) = -15.24\ m, \\ \Psi(x, z, 0) = -15.24\ m. \end{cases} \tag{21}$$

Refer to [11, 13] for more details about the expression of the analytical solution, materials and proprieties of soil used in this test problem. The L^2-error of the pressure head and the

Table 1: Evaluating pressure head and saturation L^2-errors for the proposed schemes as a function of the soil parameter $\tilde{\alpha}$ at time $T = 10$ days with $\Delta t = 5 \times 10^{-3}$ and 50×50 elements.

Method	$\alpha_v = 0.164$		$\alpha_v = 0.328$	
	L^2-error on Ψ_h	L^2-error on S_h	L^2-error on Ψ_h	L^2-error on S_h
RE-CP	0.0715341	0.00283226	1.07959	1.07959
RE-3DP	0.414159	0.0106945	1.78456	0.046826
RE-1DP	0.191474	0.00546589	0.711355	0.0232625

saturation is calculated for different schemes under various time and mesh parameters. The results (not shown here) indicate that RE-CP has a lower error compared to the other schemes. However, instability was observed when refining the mesh size and the time step, attributed to the explicit nature of the RE-CP scheme. Furthermore, RE-3DP demonstrates higher truncation errors compared to RE-1DP, which performs well and exhibits stability under variations in mesh size and time step. This highlights the improvement achieved by eliminating the need for a smoothness technique. Regarding the CPU time, RE-1DP scheme outperforms all the other schemes, as it involves computing smaller linear systems. to examine the impact of the soil parameter α_v, Table 1 presents the L^2-errors for the proposed schemes. All the schemes remain stable as α_v increases. However, as mentioned earlier, RE-3DP has a higher truncation error. The L^2-error increases as α_v is increased, which is logical because higher α_v values lead to the dominance of gravity forces over capillary forces. Conversely, RE-1DP demonstrates greater accuracy when gravity forces dominate compared to the other schemes.

4.2 TRANSPORT OF SALT IN SOIL

In the previous test, we found that RE-CP scheme has a lower error and allows for the use of the largest time step in comparison to the other schemes. For this purpose, we will adopt this technique in the predictor-corrector scheme provided in the previous section. To overcome instability issues related to this technique we will employ the predictor-corrector approach for the Richards equation (8)-(9) and the semi-implicit method for the solute transport equation

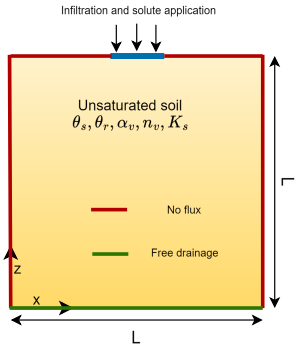

Figure 1: Schematic illustration of the test problem.

(10). This numerical test aims to assess the effectiveness of the suggested numerical approach in simulating the movement of salt in loamy soil. The numerical test evaluation is carried out in previous studies, such as [17, 11], to simulate pore-water electrical conductivity (EC) and water flow. In [17], the authors have made the dataset they used for this study available via [16]. We will compare the numerical results obtained by the suggested method with the Hydrus simulations that have been provided. The test problem is conducted within a square domain with dimensions of $2\ m \times 2\ m$. As depicted in Figure 1, a $10\ cm$ wide section is allocated at the center of the top boundary for solute application and water infiltration. The rate of water infiltration is $q_w = -0.1\ m/day$. The bottom boundary of the domain is designed to allow for free drainage, whereas the other sides are considered to have no water flow. For the solute transport, a Cauchy boundary condition is applied in the section with a constant feeding of $c = 1\, S/m$ of the inlet water. The capillary pressure and the relative hydraulic conductivity are modeled using the VG model. The test problem's parameters and material proprieties are offered as follows:

$$\begin{gathered} \theta_r = 0.078\, m^3/m^3,\ \theta_s = 0.43\, m^3/m^3,\ \alpha_v = 3.6\, m^{-1},\ n_v = 1.56, \\ K_s = 0.25\, m/day,\ \Psi_0 = -1.3\, m,\ c_0 = 0.1\, S/m,\ R = 1, \\ D_m = 0\, m^2/day,\ D_L = 0.5\, m,\ D_T = 0.1\, m, \end{gathered} \tag{22}$$

where Ψ_0 and c_0 are the initial conditions of the pressure head and salt concentration, respectively. A nonuniform triangular mesh with 4726 vertices and 9184 triangles is used to discretize the domain. We choose $\Delta t = 10^{-4}$ day as the time step, and the period of simulation is $T = 1$ day. The evolution of the solute transport, saturation, and pressure head with time is shown in Figure 2. We create a vertical cross-section of the capillary pressure and soil salt concentration solutions at the domain center ($x = 0$ m). The 1D solutions obtained are depicted in Figure 3 for two time instances, $T = 0.25$ day and $T = 0.5$ day. Favorable agreements are observed between the results obtained using the proposed scheme and those obtained with Hydrus software.

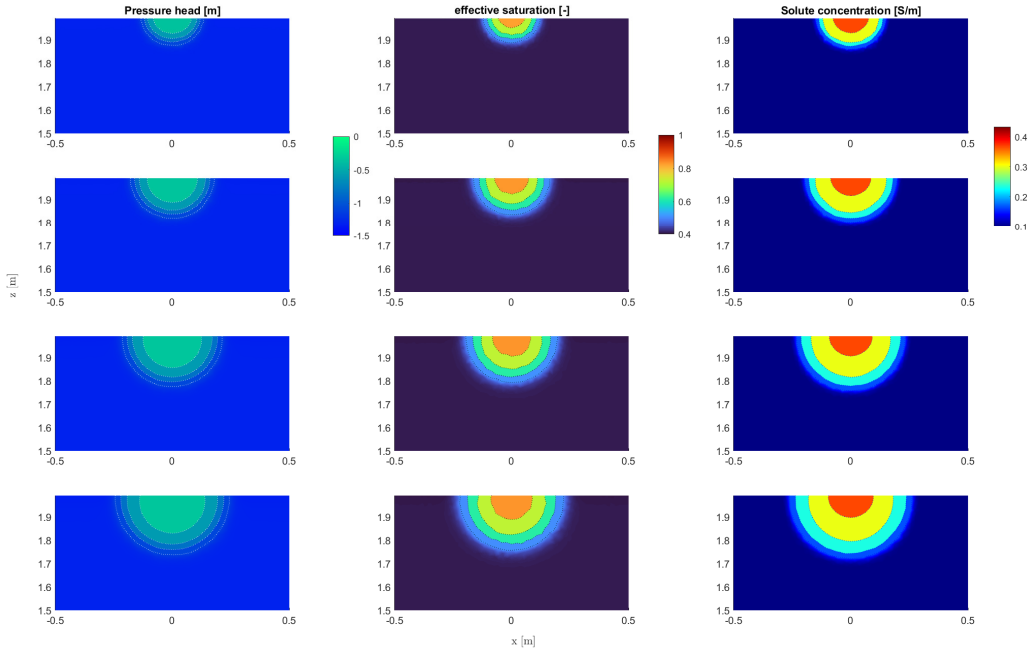

Figure 2: Time evolution of the pressure head, saturation, and solute transport for the solute transport test .

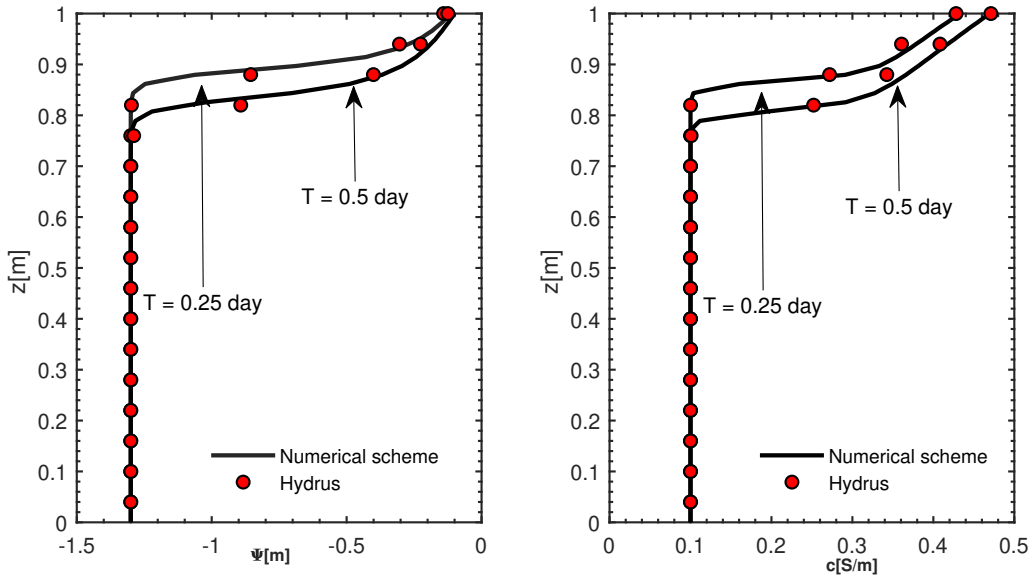

Figure 3: Cross-section of the pressure head and solute concentration at $x = 0$ of the test problem at $T = 0.25\ day$ and $T = 0.5\ day$.

5 CONCLUSION

In this study, we conducted a numerical investigation into modeling water flow and solute transport processes in unsaturated porous media. We employed an explicit predictor-corrector temporal scheme for solving the Richards equation, coupled with a mixed finite element formulation. Additionally, a semi-implicit second-order time stepping method was utilized for the advection-dispersion equation, in conjunction with the conventional finite element method in space. Furthermore, we utilized three different technique to calculate the pressure head variable in the Levrett equation, namly, RE-CP, RE-1DP and RE-3DP. The accuracy and stability of these three techniques are tested using an analytical solution of the Richards equations. While the RE-3DP scheme exhibited higher truncation error, the RE-1DP demonstrates greater accuracy when gravity forces dominate. Furthermore, The RE-CP scheme demonstrated improved accuracy, CPU time and allows for the use of the largest time step in comparison to the other schemes.

The evaluation of the proposed predictor-corrector approach with the use of RE-CP for the Leverett equation involved a practical numerical test focusing on infiltration and soil salt transport processes in loamy soil. Hydrus data served as a benchmark from existing literature. Our findings demonstrate the robustness and efficacy of the developed schemes in simulating the coupled system. Specifically, the numerical results showcased good agreement with the provided data, accurately capturing the evolution of saturation and soil salt concentration over time.

6 ACKNOWLEDGEMENT

Funding for this research was provided by Natural Sciences and Engineering Research Council of Canada, and UM6P/OCP Group of Morocco, the Moroccan Ministry of Higher Education, Scientific Research and Innovation and the OCP Foundation (APRD research program).

REFERENCES

[1] L. A. Richards, Capillary conduction of liquids through porous mediums, *Journal of Applied Physics*, 1 (1931), 318-333, doi:10.1063/1.1745010.

[2] W. R. Gardner, Some Steady State Solutions of the Unsaturated Moisture Flow Equation with Application to Evaporation from a Water Table, *Soil Science*, 85 (1958), 228-232, doi:10.1097/00010694-195804000-00006.

[3] M. Th. Van Genuchten, A closed-form equation for predicting the hydraulic conductivity of unsaturated soils, *Soil Science Society of America Journal*, 44 (1980), 892-898.

[4] S. Keita, A. Beljadid and Y. Bourgault, Implicit and semi-implicit second-order time stepping methods for the Richards equation, *Advances in Water Resources*, 148 (2021), doi:10.1016/j.advwatres.2020.103841.

[5] F. List and F. A. Radu, A study on iterative methods for solving Richards' equation, *Computational Geosciences*, 20 (2016), 341-353, doi:10.1007/s10596-016-9566-3.

[6] V. Baron, Y. Coudière and P. Sochala, Adaptive multistep time discretization and linearization based on a posteriori error estimates for the Richards equation, *Applied Numerical Mathematics*, 112 (2017), 104-125, doi:10.1016/j.apnum.2016.10.005.

[7] H. Darcy, Les Fontènes Publiques de la ville de Dijon; in: M.K. Hubert (Ed.), The Theory of Groundwater and related papers, *Hafner Pub. Co.; New York*, (1969).

[8] M. C. Levrett, Capillary behavior of porous solids, *Trans. AIME*, 142 (1941), 152-169.

[9] F. Hecht, New development in FreeFem++, *Journal of Numerical Mathematics*, 20 (2012), 251-265, doi:10.1515/jnum-2012-0013.

[10] J. Simunek, M. Sejna, and M. Th. van Genuchten, New features of version 3 of the HYDRUS (2D/3D) computer software package, *Journal of Hydrology and Hydromechanics*, 66 (2018), 133-142.

[11] N. Toutlini, A. Beljadid, and A. Soulaïmani, Analysis of second-order temporal schemes for modeling flow-solute transport in unsaturated porous media, *arXiv preprint arXiv:2404.03603*, (2024).

[12] J. Bear, *Dynamics of fluids in porous media*, Courier Corporation, (2013).

[13] H. Kamil, A. Beljadid, A. Soulaimani, and Y. Bourgault, Semi-Implicit Schemes for Modeling Water Flow and Solute Transport In Unsaturated Soils, *Advances in Water Resources*, (2024), In review.

[14] Z. L., Ö. Ilhan, and F. Z. M., A mass-conservative predictor-corrector solution to the 1D Richards equation with adaptive time control, *Journal of Hydrology*, 592 (2021), 125809, doi:10.1016/j.jhydrol.2020.125809.

[15] W. Lai, and F. L. Ogden, A mass-conservative finite volume predictor–corrector solution of the 1D Richards' equation, *Journal of Hydrology*, 523 (2015), 119-127, doi:10.1016/j.jhydrol.2015.01.053.

[16] P. Haruzi and Z. Moreno, Modeling water flow and solute transport in unsaturated soils using physics-informed neural networks trained with geoelectrical data, *Zenodo*, (2023), doi:10.5281/zenodo.7558746.

[17] P. Haruzi and Z. Moreno, Modeling Water Flow and Solute Transport in Unsaturated Soils Using Physics-Informed Neural Networks Trained With Geoelectrical Data, *Water Resources Research*, 59 (2023).